ACS OMEGA

Open Access

http://pubs.acs.org/journal/acsodf

Article

Insights into the Improved Gas Barrier Properties of Polyurethane−Clay Nanocomposite-Coated Nylon: A Solid-State NMR Study

Srinivas Chinthalapalli,* Bhuvaneswari Soundiraraju, Srirangam Siripothu, and Sushree Sangita Dash

Cite This: *ACS Omega* 2023, 8, 42144−42151

Read Online

ACCESS | Metrics & More | Article Recommendations

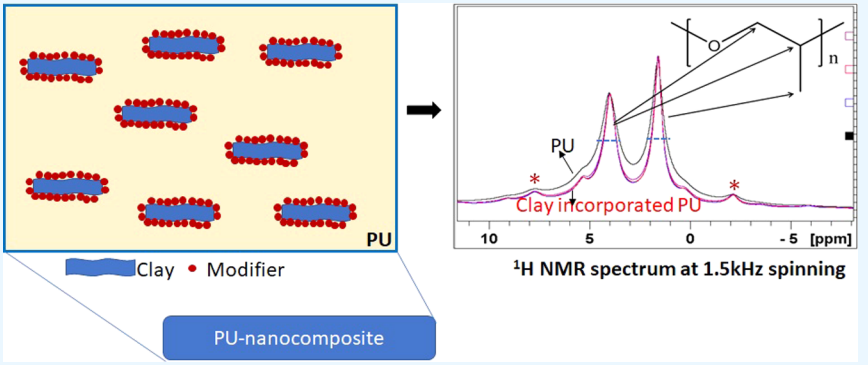

ABSTRACT: Herein, the reason for the improvement in the gas barrier properties of polyurethane (PU)−clay nanocomposite-coated nylon fabric compared to unfilled PU-coated nylon fabric is investigated by probing the changes in relaxation times of PU using solid-state nuclear magnetic resonance (SS NMR) spectroscopy. The interaction of the organically modified montmorillonite (MMT) clay (Cloisite 30B) with polyurethane (PU) in PU−clay (0.5/1/2 wt %) nanocomposites was probed with respect to the change in the spin−lattice relaxation time of protons in the PU chain due to the presence of paramagnetic species in clay (T_{1H}, para). The better the dispersion of the clay in the PU matrix, the lower the T_{1H}, para, due to the interaction between clay and the PU matrix. 0.5 wt % PU−clay has lower T_{1H}, para, (6.4 s) compared to 1 wt % (18.3 s) and 2 wt % (14.3 s) filled systems. The SS NMR findings are in good agreement with field-emission scanning electron microscopy (FE-SEM) analyses. In SEM microscopic images, it is observed that the PU−0.5 wt % clay has better exfoliation of clay compared to the 1 and 2 wt % PU−clay nanocomposites. This is in agreement with improved gas barrier properties of the nanocomposite coated on the nylon fabric for 0.5 wt % clay (2300 mL/m^2/day) compared with 1 wt % (2500 mL/m^2/day) and 2 wt % clay (2600 mL/m^2/day)-incorporated PU-coated fabrics and neat PU-coated nylon fabric (4500 mL/m^2/day) at 260 GSM.

1. INTRODUCTION

Solid-state (SS) NMR plays a vital role in characterizing polymer nanocomposites as it shows the nature of interaction and extent of dispersion of the filler in the polymer matrix.[1] NMR parameters such as chemical shift, line width, line shape, and relaxation times depend on the local structure and dynamics of the polymer unit/chain in the composite, which influence its macroscopic properties.[2] The relaxation time of nuclei is the time taken for the magnetization of a particular nucleus to attain equilibrium after their excitation. The relaxation of nuclei is majorly classified into three types: spin−lattice relaxation time in the laboratory frame (T_1), spin−lattice relaxation time in the rotating frame ($T_{1\rho}$), and spin−spin relaxation time (T_2). Based on the polymer system and the type of clay added, one of these relaxation times or the other NMR parameters can be affected. These NMR studies were employed to study the structure−property relationship of various polymer nanocomposites.[3−10]

Polymer nanocomposites contain polymeric materials as the matrix along with a filler where at least one of the dimensions of the filler is in the nanometer size range.[11] Layered silicate clays, such as montmorillonite (MMT), are the most widely used fillers, which are added to the polymer matrix in small fractions to improve the physical properties such as tensile strength, modulus, and gas barrier properties.

Received: May 24, 2023
Revised: September 26, 2023
Accepted: October 10, 2023
Published: November 2, 2023

https://doi.org/10.1021/acsomega.3c03657
ACS Omega 2023, 8, 42144−42151

Scheme 1. Synthesis of the Cured Polyurethane

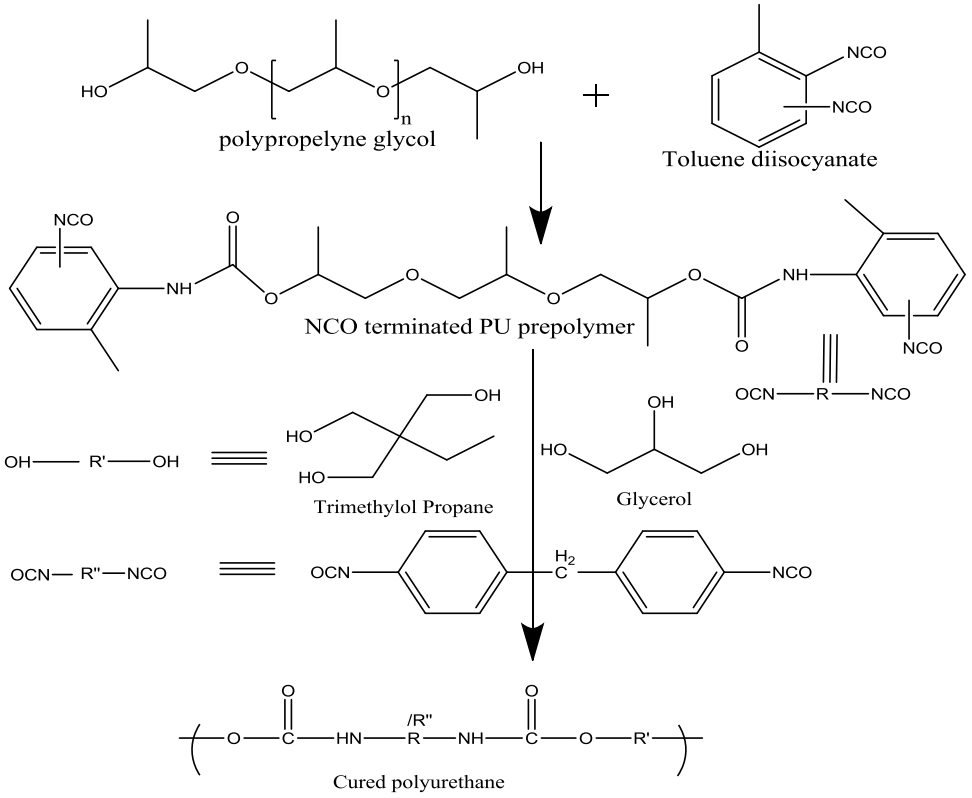

MMTs are composed of a silica tetrahedral surface and octahedrally coordinated Al^{3+} as the central plane with a small amount of substituents, such as Mg^{2+} and Fe^{3+}. The presence of Mg^{2+} endows clay with a net negative charge, which can be neutralized with other cations such as Na^{+} or organic cations such as tetrasubstituted ammonium for better interaction of clay with the polymer matrix.[12] The Fe present in the clay, termed paramagnetic impurity, is low in concentration, and its direct influence can be observed only on the nearby ^{1}H network surrounding the clay. Because of the large dipole−dipole interaction between proton nuclei, the paramagnetic effect is carried to other protons through diffusion, leading to the shortening of the proton spin−lattice relaxation time constant (T_{1H}), which depends on the concentration of Fe in the clay layer and the average distance between the layers.[13−15] The latter dependence provides insights into the quality of clay dispersion.[16] The paramagnetic effect is found to be a useful probe in characterizing the clay dispersion within the polymer matrix of the polymer nanocomposites.[17] VanderHart et al. used T_{1H} to probe the dispersion of MMT in the nylon polymer matrix,[18,19] and similarly, Xu et al. used these relaxation parameters to probe the degree of exfoliation of MMT in polypropylene MMT nanocomposites.[20]

On the other hand, polyurethane (PU) clay nanocomposite studies were reported with respect to the enhancement in PU macroscopic properties.[21−23] Wang et al.[22] used X-ray diffraction (XRD) measurements to determine the enhancement in the mechanical properties of PU−organically modified clay nanocomposites based on the increase in the chain length of the organic modifier, which is proportional to the gallery expansion. Similarly, Strankowski et al.[23] reported an enhancement of the thermal and mechanical properties of PU−clay composites on the addition of 1 wt % organically modified MMT (Cloisite 10A and 20A) due to intercalation and partial exfoliation of clay when probed by XRD. Xiong et al.[24] examined the microstructure of the PU−organically modified clay (MMT with methylene-bis-ortho-chloroaniline) nanocomposites with different contents of clay by atomic force microscopy (AFM) and correlated with the thermal and mechanical properties of PU. Adak et al.[25] studied the gas barrier properties of a PU−clay (Cloisite 30B) nanocomposite film by varying the processing conditions and showed the possible intercalation/exfoliation of clay by using XRD, SEM, and transmission electron microscopy (TEM) techniques.

However, investigations of PU−clay nanocomposites by employing solid-state NMR are scarce. Here, we envisage a PU coating over nylon fabric as the former has better gas barrier properties than silicones and easier processability than polychlorotrifluoroethylene (PCTFE)−poly(tetrafluoroethylene) (PTFE) systems, while the latter has good mechanical strength and stretchability over polyester fabrics. Coating of the PU−clay nanocomposite onto a nylon fabric is adopted to further enhance the gas barrier properties of the nylon fabric. The obtained fabric will be used in space applications for space suites, pressure bladder material, etc. In this regard, solid-state NMR studies using proton T_1 (T_{1H}) were effectively employed as a tool to determine the quality of dispersion of clay (Cloisite 30B with 0.5/1/2 wt %) in the PU nanocomposite and the resulting gas barrier properties. Proton T_2 (T_{2H}) measurements were performed to determine the diffusion coefficient of the PU nanocomposite. NMR studies of the PU nanocomposites before choosing the coating formulation provide insights into the amount of nanoclay required to achieve the improved barrier property.

https://doi.org/10.1021/acsomega.3c03657
ACS Omega 2023, 8, 42144−42151

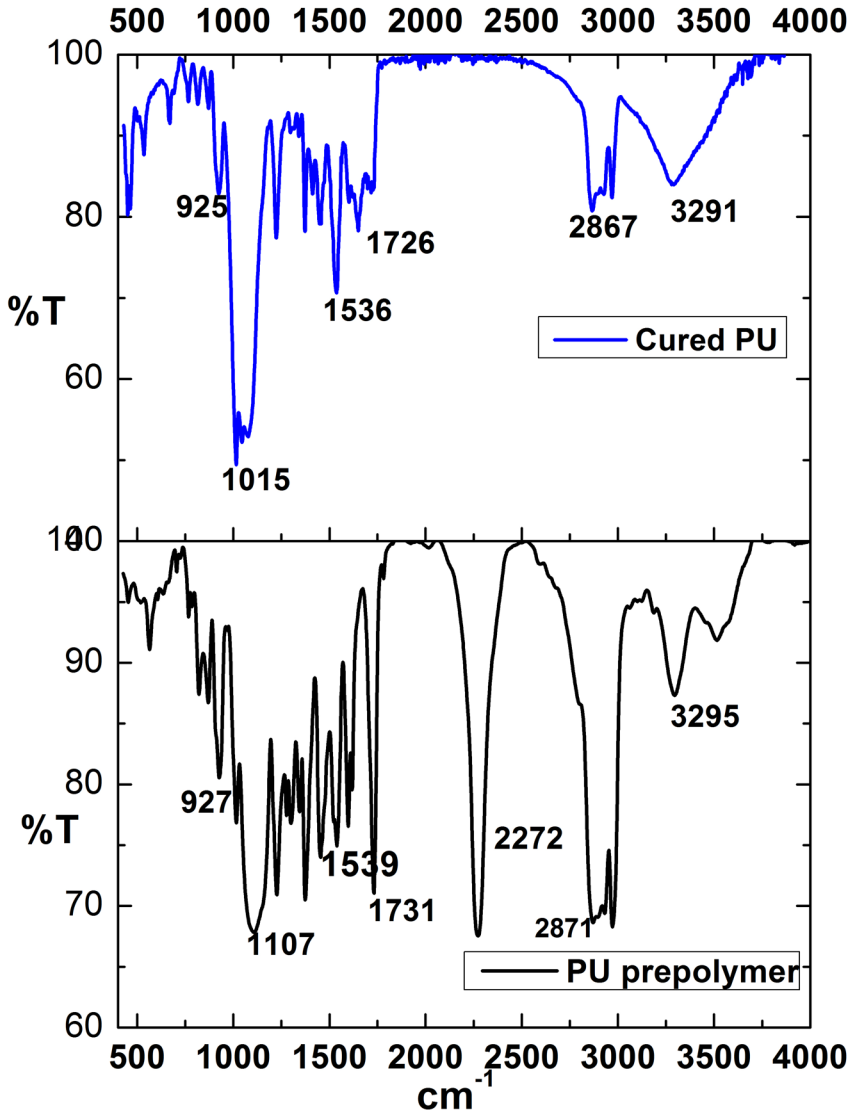

Figure 1. Overlaid FTIR spectra of the PU prepolymer (bottom) and cured polyurethane (top).

The preliminary NMR study also reduces the number of trials required for coating and eliminates the requirement for macroscopic testing of each composition.

2. EXPERIMENTAL SECTION

2.1. Materials. Polypropylene glycol (PPG; −OH value = 54.5; M_n = 1900) and 2,4- and 2,6-toluene diisocyanate (80:20) (TDI, %NCO = 99.16) were obtained from M/s Lab Chemie Industries, Mumbai. 4,4′-Diphenylmethane diisocyanate (MDI, %NCO = 32) was received from M/s Surabhi chemicals, Mumbai. Clay (Cloisite 30B) (specific gravity = 1.98 g/cm^3) was procured from M/s Southern Clay, Mumbai, and used as received.

2.2. Preparation of the NCO-Terminated PU Prepolymer/PU Prepolymer. To the vacuum-dried polypropylene glycol (1 kg), *n*-propyl alcohol (0.125 wt %) and *n*-propyl iodide (0.125 wt %) catalyst are added and mixed thoroughly. A stoichiometric amount of toluene diisocyanate (20 wt %) is added slowly with thermal control and in an inert atmosphere. The temperature is maintained at 70 °C under stirring. The reaction is continued for 4 h under temperature control. After the reaction, it is cooled to room temperature, discharged into containers, stored under a nitrogen atmosphere, and sealed. The final resin is named NCO-terminated PU prepolymer (η = 2690 cps at 30 °C).

2.3. Preparation of the Crosslinking System. A 60:40 (wt %) mixture of 1,1,1-trimethylol propane and glycerol is used as a crosslinking agent. The mixture is dried under vacuum and 0.3 wt % dibutyl tin dilaurate (DBTDL) is added.

2.4. Preparation of the Clay-Incorporated PU Prepolymer. The clay (0.5/1/2 wt %) is dispersed in toluene (100 mL) through ultrasonication for 45 min, and then the PU prepolymer (100 g) is added. The solution is again ultrasonicated for 45 min to facilitate the intercalation of polymer chains between the clay layers. The nanocomposite is obtained by solvent removal through vaporization at RT while being coated over the fabric. Ultrasonication is performed at a frequency of 20,000 Hz, a maximum amplitude of 40%, and a maximum temperature of 50 °C.

2.5. Preparation of the Coating Formulation. A 100 g portion of clay-incorporated PU prepolymer is weighed in a beaker. 3.5 g of the crosslinker is added and stirred with a

https://doi.org/10.1021/acsomega.3c03657
ACS Omega 2023, 8, 42144−42151

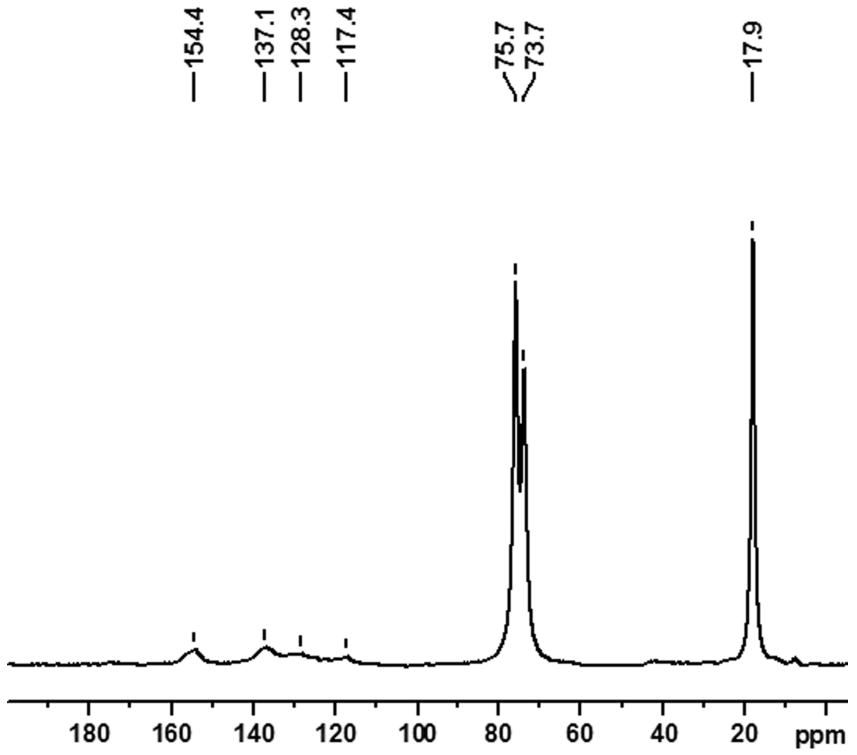

Figure 2. ^{13}C CP MAS NMR of cured PU with 10 kHz spinning.

glass rod for 5 min. 7g of MDI is added to the mixture and stirred once again. It can be applied either by brushing or by spraying by adding 100 mL of toluene. After coating, it is kept for partial curing for 24 h. Then, a second coating is performed and allowed to cure for 48 h at ambient conditions. To confirm the coating thickness, the coated fabric (1 m^2) was cut into 20 pieces at different locations, and the thickness was measured using a calibrated thickness gauge whose value was 240 ± 10 μm, out of which five specimens were used for gas permeability testing.

Scheme 1 shows the steps involved in the synthesis of polyurethane.

3. CHARACTERIZATION

3.1. Fourier Transform-Infrared (FTIR) Spectroscopy. The IR spectrum of the cured polyurethane sample was recorded using a Thermofischer Scientific Nicolet iS50 FTIR spectrometer in ATR mode using a universal diamond ATR. The NCO-terminated PU prepolymer was taken by smearing the sample in between two KBr plates, and the FTIR spectrum was recorded in the range of 4000−400 cm^{-1} at a resolution of 4 cm^{-1}.

3.2. Inductively Coupled Plasma Atomic Emission Spectroscopy (ICP-AES). ICP analysis to estimate the iron content was carried out using PerkinElmer Optima 4300 V ICP-AES. Samples were dissolved by acid digestion/sodium carbonate fusion and aspirated to argon plasma.

3.3. SS NMR Spectroscopy. The measurements were conducted using a 400 MHz (with respect to 1H) Bruker Avance III HD spectrometer operating at 9.4 T. The sample is filled in a 4 mm rotor. The ^{13}C cross-polarization (CP) magic-angle spinning (MAS)[26] experiments were conducted using 3 ms CP time, 10 kHz magic-angle spinning (MAS) frequency, ν_r, and a repetition time of 5 s. Saturation recovery experiments were conducted to measure the time period associated with the recovery of the signal, and it was found that a relaxation delay of 7 s is satisfactory to carry out inversion recovery experiments[27] to probe T_{1H} and Carr−Purcell−Meiboom−Gill (CPMG) experiments[28,29] to probe T_{2H}. The experiments were carried out with a 90° pulse of 4.35 μs, at an acquisition time of 25 ms, with the number of scans = 8 and ν_r = 0 kHz.

3.4. Differential Scanning Calorimetry (DSC). DSC analysis of the samples was carried out using a TA Instruments 2920 MDSC under a 99.999% argon atmosphere purged at a flow rate of 50 mL/min. Approximately 5 mg of the sample was taken in an aluminum pan and heated from −80 to +30 °C at a heating rate of 10 °C/min.

3.5. FE-SEM. SEM images were recorded in a Carl Zeiss Gemini SEM 500 field-emission scanning electron microscope at an acceleration voltage of 15 kV using a secondary electron detector. The sample was sputtered with a conductive layer of gold/palladium before SEM imaging. Energy-dispersive X-ray spectral (EDS) analysis was carried out using a Bruker Quantax Xflash60 energy-dispersive X-ray spectrometer at an acceleration voltage of 15 kV.

3.6. Helium Gas Permeability Analyzer. The helium permeability of the PU nanocomposite-coated nylon-6 fabric was measured at room temperature using a PBI Dansensor Lyssy L100−5000 manometric gas permeability analyzer. The instrument employs the manometric principle: the pressure change via gas transmission through the fabric is observed. Five specimens were used to evaluate the helium gas permeability in each category. The results are expressed in $mL/m^2/day$.

https://doi.org/10.1021/acsomega.3c03657
ACS Omega 2023, 8, 42144−42151

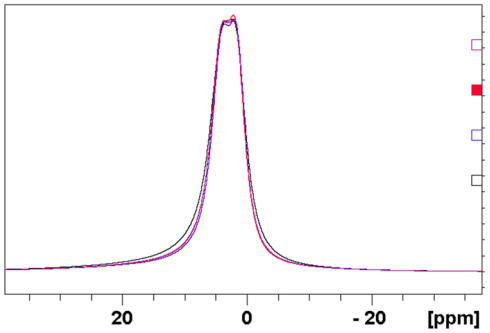

Figure 3. ^{1}H NMR overlay of cured PU (black) and clay-incorporated PU systems (0.5 wt % NC, blue; 1 wt % NC, red; and 2 wt % NC, violet) at 0 kHz spinning.

4. RESULTS AND DISCUSSION

4.1. FTIR Spectral Analysis. The overlaid spectra of the PU prepolymer and cured polyurethane are shown in Figure 1.

The peak at 1725−1735 cm^{-1} corresponds to C═O stretching, 1015−1110 cm^{-1} to C−O stretching, 3295 cm^{-1} to − NH stretching, 1539 cm^{-1} to in-plane N−H bending of urethane and 2865−2875 cm^{-1} to aliphatic C−H stretching. The peak at 2272 cm^{-1} corresponds to NCO stretching, which disappeared in the cured PU and shows the completion of the reaction.

4.2. ICP-AES Analysis. From the analysis, the weight percentage of iron in the clay was found to be 2.3.

4.3. SS NMR Analysis. The ^{13}C CP MAS NMR spectrum of cured PU is shown in Figure 2.

As the PPG fraction (peaks at 17.9, 73.7, and 75.7 ppm) is very high due to its polymeric nature compared to that of the isocyanate portion (aromatic peaks at 117.4 128.3, 137.1, and 154.4 ppm), as evident from the ^{13}C CP MAS NMR spectrum, the relaxation parameters of the PPG portion were probed using ^{1}H NMR spectroscopy by an inversion recovery experiment. The ^{1}H NMR overlay of the cured PU and clay-incorporated PUs is given in Figure 3.

Compared to unfilled PU, the ^{1}H NMR spectral lines of clay-incorporated PUs are narrower. This shows that the presence of the filler makes the matrix system comparatively flexible, which increases the coherence time of the signal decay, resulting in line narrowing.

Table 1. PU nanocomposites $T_{1H,\,neat}$, $T_{1H,\,composite}$, and deduced $T_{1H,\,para}$ at 0 kHz spinning and 300 K

	at 2.1 ppm[a]		
PU with cloisite 30B	$T_{1H,neat}$ (ms)	$T_{1H,composite}$ (ms)	$T_{1H,para}$ (s)
0 wt %	777.7 ± 3.3	N/A	N/A
0.5 wt %	N/A	693.3 ± 3.7	6.4 ± 1.0
1 wt %	N/A	746.0 ± 2.0	18.3 ± 0.6
2 wt %	N/A	737.7 ± 3.7	14.3 ± 0.3

[a]Average value of experiments and associated error.

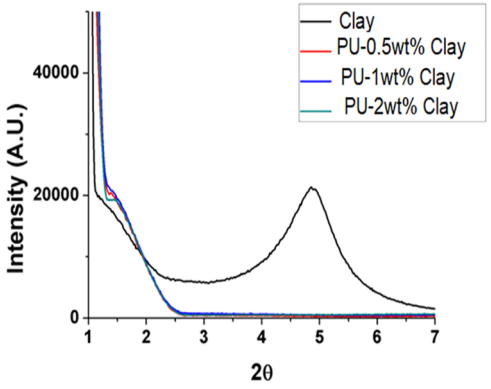

Figure 5. Overlaid XRD diffractograms of clay and clay-filled PU nanocomposites.

To further prove the observation, the DSC of PU was recorded without and with 0.5 wt % clay, which is shown in Figure 4.

Compared to PU, the glass transition temperature of the 0.5 wt % clay-incorporated PU decreased as observed earlier for polyurethane−clay nanocomposites[30] and poly(L-lactic acid)−organically modified vermiculite nanocomposites,[31] which was attributed to the plasticizing effect of the organic moiety present in the clay, which confirms the NMR observations.

Clay is paramagnetic due to the presence of iron (2.3 wt %), as reflected by ICP-AES measurements. The content of iron in the filler is sufficient to induce spin−lattice relaxation of protons present in the matrix, which is termed as the spin−lattice relaxation time constant due to the paramagnetic component, $T_{1H,para}$.[32] Here, the $T_{1H,para}$ parameter is used to

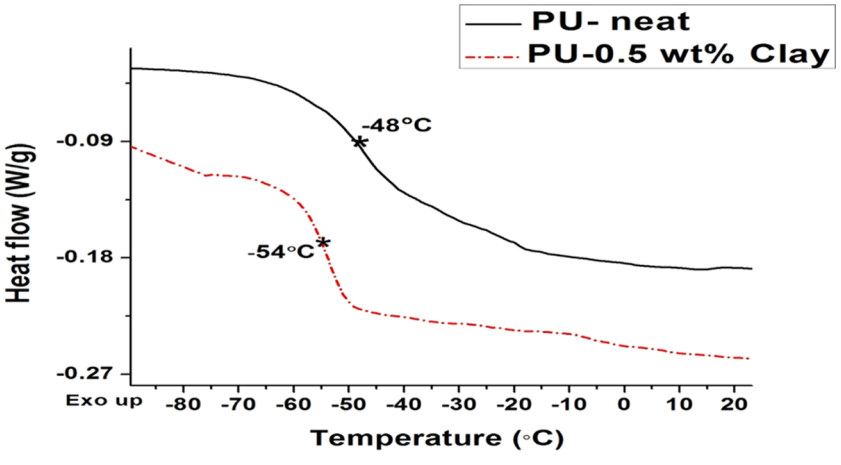

Figure 4. DSC overlay of PU and PU with 0.5 wt % clay.

https://doi.org/10.1021/acsomega.3c03657
ACS Omega 2023, 8, 42144−42151

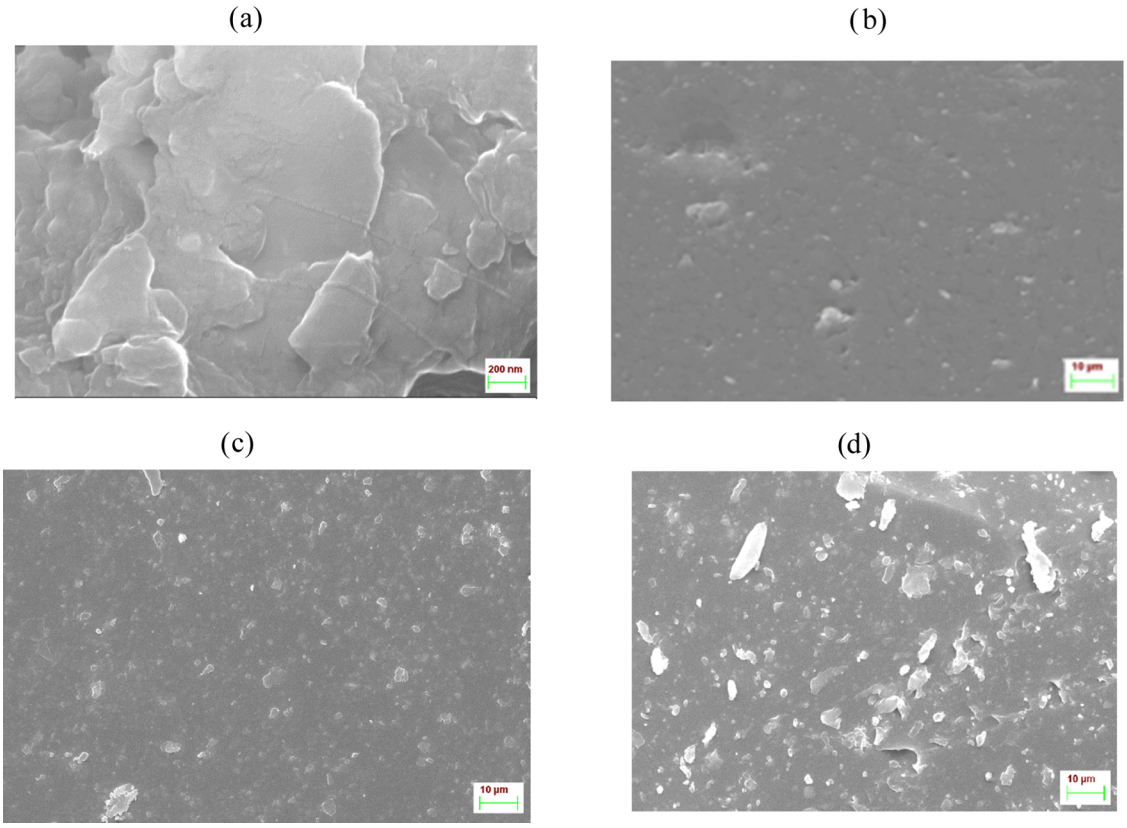

Figure 6. SEM images of PU nanocomposites: (a) fillers at higher magnification for 0.5 wt % clay, (b) 0.5 wt % clay, (c) 1 wt % clay, and (d) 2 wt % clay.

Table 2. Gas Permeability of the Nylon-6,6 Fabric Coated by the PU Composite

clay wt % in PU	gas permeability (mL/m^2/day) for PU-coated nylon fabric @ 260 ± 10 GSM[a]
0	4506 ± 114
0.5	2300 ± 110
1	2513 ± 98
2	2589 ± 116

[a]Average value of experiments and the associated error.

probe the filler dispersion in the matrix, which is calculated as shown in eq 1, and the values are given in Table 1.

$$\frac{1}{T_{1H,para}} = \frac{1}{T_{1H,composite}} - \frac{1}{T_{1H,neat\ PU}} \quad (1)$$

The validity of eq 1 is satisfied by the following four factors:[20] (i) sufficient amount of paramagnetic impurities are present in the clay (2.3 wt % iron), which is in the similar range of available organoclays; (ii) the polymer has a moderate amount of clay: 0.5−2 wt %; (iii) no significant changes are observed in the morphology of the polymer matrix by the addition of clay (in the following section from SEM analyses), which does not change $T_{1H,neat}$; and (iv) the spin diffusion coefficient (D) is optimal to induce magnetization of nearby protons as shown below:

D is derived from the empirical relation obtained by Mellinger et al.[33] as follows:

$$D(T_2^{-1}) = (4.4 \times 10^{-5} T_2^{-1} + 0.26)\ \text{nm}^2/\text{ms},$$
$$1000\,\text{Hz} < T_2^{-1} < 3500\,\text{Hz} \quad (2)$$

The T_2^{-1} value obtained from the CPMG experiment is 1526 ± 26 Hz for the 0.5 wt % clay-incorporated PU composite, between 1000 and 3500 Hz. Therefore, eq 2 can be employed to calculate D, and the value obtained is 0.33 nm^2/ms. D values about this range are sufficient to induce magnetization with nearby protons.

The lower the $T_{1H,para}$, the better the dispersion.[32] Here, PU with 0.5 wt % clay has a lower $T_{1H,para}$ compared to 1 and 2 wt % clay, which implies better dispersion of the former compared to the latter.

4.4. XRD analysis. The overlay of the X-ray diffractograms is shown in Figure 5.

The clay peak is observed at 2θ = 4.8°. The peak is absent in the clay-filled PU composites. This might be due to the total destruction of clay in the polymer matrix (exfoliated nanocomposites) or because the clay content is too low to be detected in the diffractogram.

4.5. FE-SEM Analyses. The NMR results are validated with EDS elemental mapping for filler loadings of 0.5, 1, and 2 wt %, as shown in Figure 6.

Figure 6a shows that PU filled with 0.5 wt % has thin flakes of clay. Figure 6b−6d displays a comparison of the dispersion of the clay for PU filled with 0.5, 1, and 2 wt % clay. The agglomeration tendency of clay particles is increased beyond 0.5 wt % clay addition, but the morphology of the polymer matrix has not changed. The better exfoliation of clay in 0.5 wt % clay-incorporated PU nanocomposites leads to the lower gas permeability of the coated nylon fabric (Table 2) due to an increase in the tortuous path for the diffusing molecules.[34]

4.6. Gas Permeability Measurements. See Table 2.

https://doi.org/10.1021/acsomega.3c03657
ACS Omega 2023, 8, 42144−42151

5. CONCLUSIONS

The iron present in clay induces the relaxation of protons of PU through diffusion due to the large dipolar interactions between the protons, called paramagnetic relaxation, which is used as the probe for assessing the quality of clay dispersion in the polyurethane matrix. Here, the 0.5 wt % clay-incorporated PU nanocomposite exhibits better clay dispersion, causing faster relaxation of protons compared to the 1 and 2 wt % filled systems. The results are further supported by FE-SEM analyses of the PU composites and gas barrier properties of the PU-coated fabric, as better exfoliation leads to an increase in the tortuosity of the gas molecules.

AUTHOR INFORMATION

Corresponding Author

Srinivas Chinthalapalli − *Analytical and Spectroscopy Division, Analytical, Spectroscopy and Ceramics Group, PCM Entity, Vikram Sarabhai Space Centre (VSSC), Thiruvananthapuram 695022, India;* orcid.org/0000-0003-1855-6421; Email: cnuvas2006@gmail.com

Authors

Bhuvaneswari Soundiraraju − *Lasers Systems and Instrumentation Group, Photonics Systems Area, Laboratory for Electro-Optics Systems, Bengaluru 560058, India;* orcid.org/0000-0001-8531-8904

Srirangam Siripothu − *Propellant Fuel Complex, Energy Systems Group, PCM Entity, Vikram Sarabhai Space Centre (VSSC), Thiruvananthapuram 695022, India*

Sushree Sangita Dash − *Propellant Fuel Complex, Energy Systems Group, PCM Entity, Vikram Sarabhai Space Centre (VSSC), Thiruvananthapuram 695022, India*

Complete contact information is available at: https://pubs.acs.org/10.1021/acsomega.3c03657

Notes

The authors declare no competing financial interest.

ACKNOWLEDGMENTS

The authors acknowledge the Director VSSC for giving permission to publish this work, DD/PCM for research support, Propellant Fuel Complex/VSSC for providing research facilities, Analytical Spectroscopy Division/VSSC for ICP-AES, XRD, and FE-SEM measurements, Dr. Dona Mathew, PSCD/VSSC, Dr. Jayanthi S from IIST and reviewer of ACS Omega for critical review, and IIST, Trivandrum test facility, for helium gas permeability measurements.

REFERENCES

(1) Blümich, B. *NMR Imaging of Materials*; Clarendon Press: Oxford, UK, 2000.

(2) Brown, S. P.; Spiess, H. W. Advanced Solid-State NMR Methods for the Elucidation of Structure and Dynamics of Molecular, Macromolecular, and Supramolecular Systems. *Chem. Rev.* **2001**, *101* (12), 4125−4156.

(3) Lino, A. S.; Mendes, L. C.; Silva, D. F.; Malm, O. High Density Polyethylene and Zirconium Phosphate Nanocomposites. *Polímeros* **2015**, *25* (5), 477−482.

(4) Mayer, B. P.; Chinn, S. C.; Maxwell, R. S.; Reimer, J. A. Solid state NMR investigation of γ-irradiated composite siloxanes: Probing the silica/polysiloxane interface. *Polym. Degrad. Stab.* **2013**, *98* (7), 1362−1368.

(5) Eckman, R. R.; Henrichs, P. M.; Peacock, A. J. Study of Polyethylene by Solid State NMR Relaxation and Spin Diffusion. *Macromolecules* **1997**, *30* (8), 2474−2481.

(6) Peng, W.; Feng, C.; Hou, J.; Zhang, R.; Sun, P.; Gao, Y.; Wang, X. Probing the Dynamic Structural Evolution of End-Functionalized Polybutadiene/Organo-Clay Nanocomposite Gels before and after Yielding by Nonlinear Rheology and ^{1}H Double-Quantum NMR. *Polymers* **2022**, *14* (8), 1518.

(7) Bokobza, L. Spectroscopic Techniques for the Characterization of Polymer Nanocomposites: A Review. *Polymers* **2018**, *10* (1), 7.

(8) Borsacchi, S.; Sudhakaran, U.; Ruggeri, G.; et al. Synthesis, Characterization, and Solid-State NMR Investigation of Organically Modified Bentonites and Their Composites with LDPE. *Langmuir* **2013**, *29* (29), 9164−9172.

(9) Avolio, R.; Gentile, G.; Errico, M. E.; et al. Synthesis and Characterization of Poly(methylmethacrylate)/Silica Nanocomposites: Study of the Interphase by Solid-State NMR and Structure/Properties Relationships. *J. Polym. Sci., Part A − Polym. Chem.* **2010**, *48* (23), 5618−5629.

(10) da Silva, E. O.; Tavares, M. I. B.; Nogueira, J. S. Solid State NMR Evaluation of Natural Resin/Clay Nanocomposites. *J. Nano Res.* **2009**, *4*, 117−126.

(11) Pavlidou, S.; Papaspyrides, C. D. A Review on Polymer−Layered Silicate Nanocomposites. *Prog. Polym. Sci.* **2008**, *33* (12), 1119−1198.

(12) Dombrowski, T. *Encyclopedia of Chemical Technology*, 4th ed.; John Wiley & Sons: New York, 1993; Vol. *6*, pp 381−405.

(13) Blumberg, W. E. Nuclear Spin-Lattice Relaxation Caused by Paramagnetic Impurities. *Phys. Rev.* **1960**, *119*, 79.

(14) Abragam, A. *The Principles of Nuclear Magnetism*; Oxford University Press: New York, 1961, Chapter V.

(15) Hayashi, S.; Akiba, E. Nuclear spin-lattice relaxation mechanisms in kaolinite confirmed by magic angle spinning. *Solid State Nucl. Magn. Reson.* **1995**, *4*, 331−340.

(16) VanderHart, D. L.; Gilman, J. W.; Asano, A. NMR Measurements Related to Clay-Dispersion Quality and Organic-Modifier Stability in Nylon-6/Clay Nanocomposites. *Macromolecules* **2001**, *34* (12), 3819−3822.

(17) Grandjean, J. Solid-State NMR Study of Modified Clays and Polymer/Clay Nanocomposites. *Clay Miner.* **2006**, *41*, 567−586.

(18) VanderHart, D. L.; Asano, A.; Gilman, J. W. Solid-State NMR Investigation of Paramagnetic Nylon-6 Clay Nanocomposites. 1. Crystallinity, Morphology, and the Direct Influence of Fe3+ on Nuclear Spins. *Chem. Mater.* **2001**, *13* (10), 3781−3795.

(19) VanderHart, D. L.; Asano, A.; Gilman, J. W. Solid-State NMR Investigation of Paramagnetic Nylon-6 Clay Nanocomposites. 2. Measurement of Clay Dispersion, Crystal Stratification, and Stability of Organic Modifiers. *Chem. Mater.* **2001**, *13* (10), 3796−3809.

(20) Xu, B.; Leisen, J.; Boehme, U.; Scheler, U.; Beckham, H. W. ^{1}H NMR T_1 Relaxation of Polymer/Montmorillonite Nanocomposites with Different Clay Contents and Degrees of Exfoliation: Magnetic Field Effects. *Z. Phys. Chem.* **2012**, *226*, 1229−1241.

(21) Boulaouche, T.; Kherroub, D. E.; Benzerafa, A.; Khimeche, K.; Belbachir, M. New Synthesis of Polyurethane Nanocomposites based on Maghnite used both as a Catalyst and as an Inorganic Improver of Thermal, Mechanical and Textural Properties. *J. Mater. Res. Technol.* **2020**, *9* (6), 15222−15232.

(22) Wang, Z.; Pinnavaia, T. J. Nanolayer Reinforcement of Elastomeric Polyurethane. *Chem. Mater.* **1998**, *10* (12), 3769−3771.

(23) Strankowski, M.; Strankowska, J.; Gazda, M.; Piszczyk, L.; Nowaczyk, G.; Jurga, S. Thermoplastic Polyurethane/(Organically Modified Montmorillonite) Nanocomposites Produced by In Situ Polymerization. *Express Polym. Lett.* **2012**, *6* (8), 610−619.

(24) Xiong, J.; Zheng, Z.; Jiang, H.; Ye, S.; Wang, X. Reinforcement of Polyurethane Composites with an Organically Modified Montmorillonite. *Composites, Part A* **2007**, *38* (1), 132−137.

(25) Adak, B.; Mangala, J.; Bhupendra, S. B. Polyurethane/Clay Nanocomposites with Improved Helium Gas Barrier and Mechanical

Properties: Direct versus master-batch melt mixing route. *J. Appl. Polym. Sci.* **2018**, *135*, 46422.
(26) Schaefer, J.; Stejskal, E. O.; Buchdahl, R. Magic-Angle ^{13}C NMR Analysis of Motion in Solid Glassy Polymers. *Macromolecules* **1977**, *10* (2), 384−405.
(27) Farrar, T. C.; Becker, E. D. *Pulse and Fourier Transform NMR*; Academic Press: New York, 1971; p 20f.
(28) Carr, H. Y.; Purcell, E. M. Effects of Diffusion on Free Precession in Nuclear Magnetic Resonance Experiments. *Phys. Rev.* **1954**, *94*, 630 DOI: 10.1103/PhysRev.94.630.
(29) Meiboom, S.; Gill, D. Modified Spin-Echo Method for Measuring Nuclear Relaxation Times. *Rev. Sci. Instrum.* **1958**, *29*, 688−691, DOI: 10.1063/1.1716296.
(30) Białkowska, A.; Krzykowska, B.; Zarzyka, I.; Bakar, M.; Sedlarik, V.; Kovarova, M.; Czerniecka-Kubicka, A. Polymer/Layered Clay/Polyurethane Nanocomposites: P3HB Hybrid Nanobiocomposites-Preparation and Properties Evaluation. *Nanomaterials* **2023**, *13* (2), 225.
(31) Fernández, M. J.; Dolores, F. M.; Aranburu, I. Poly(l-Lactic acid)/Organically Modified Vermiculite Nanocomposites Prepared by Melt Compounding: Effect of Clay Modification on Microstructure and Thermal Properties. *Eur. Polym. J.* **2013**, *49* (6), 1257−1267.
(32) Powers, D. S.; Vaia, R. A.; Koerner, H.; Serres, J.; Mirau, P. A. NMR Characterization of Low Hard Segment Thermoplastic Polyurethane/Carbon Nanofiber Composites. *Macromolecules* **2008**, *41* (12), 4290−4295.
(33) Mellinger, F.; Wilhelm, M.; Spiess, H. W. Calibration of 1H NMR spin diffusion coefficients for mobile polymers through transverse relaxation measurements. *Macromolecules* **1999**, *32*, 4686−4691.
(34) Nielsen, L. E. Models for the permeability of filled polymer systems. *J. Macromol. Sci., Part A* **1967**, *1* (5), 929−942.

https://doi.org/10.1021/acsomega.3c03657
ACS Omega 2023, 8, 42144−42151